SUPPLEMENTARY INFORMATION

5-Methyl-*N*-(8-(5,6,7,8-tetrahydroacridin-9-ylamino)octyl)-5*H*-indolo[2,3-*b*]quinolin-11-amine: A Highly Potent Human Cholinesterase Inhibitor

Li Wang,[a] Ignacio Moraleda,[b] Isabel Iriepa,[b] Alejandro Romero,[c] Francisco López-Muñoz,[d,e] Mourad Chioua,[f] Tsutomu Inokuchi,[a,*] Manuela Bartolini,[g,*] and José Marco-Contelles[f,*]

[a]*Division of Chemistry and Biotechnology, Graduate School of Natural Science and Technology, Okayama University, 3.1.1 Tsushima-Naka, Kita-ku, Okayama 700-8530, Japan.*
[b]*Departamento de Química Orgánica y Química Inorgánica. Universidad de Alcalá, Ctra. Madrid-Barcelona, Km. 33,6, 28871, Alcalá de Henares, Madrid, Spain.*
[c]*Departamento de Toxicología y Farmacología, Facultad de Veterinaria, Universidad Complutense de Madrid, 28040-Madrid, Spain*
[d]*Faculty of Health, Camilo José Cela University, C/ Castillo de Alarcón, 49; 28692 Villanueva de la Cañada, Madrid, Spain*
[e]*Neuropsychopharmacology Unit, "Hospital 12 de Octubre" Research Institute, Av. de Córdoba s/n, 28041 Madrid, Spain*
[f]*Laboratory of Medicinal (IQOG, CSIC), C/ Juan de la Cierva 3, 28006-Madrid, Spain*
[g]*Department of Pharmaceutical Sciences, Alma Mater Studiorum, University of Bologna, Via Belmeloro 6, 40126 Bologna, Italy*

CONTENT

1. Synthesis of compounds 1-3…….S2-S5

2. Biological evaluation……S6-S7

3. Docking analysis……S8-S13

4. ADME of tacrine-neocryptolepine derivatives 1-3……..S14

5. Inhibition of amyloid self-aggregation…….……S15

6. References…….S16

1. Synthesis of compounds 1-3

General Methods. The starting materials anthranilic acid, cyclohexanone, diamines, $POCl_3$, phenol, NaI and solvents were commercially available, which were directly used as received without purification. The ^1H NMR and ^{13}C NMR spectra were taken on the Varian INOVA-600 or Varian INOVA-400 spectrometer, and the HRMS data were taken on the Shimadzu LCMS-IT-TOF.

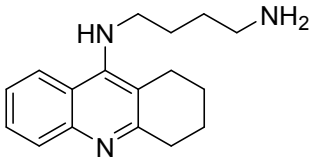

***N*-(4-aminobutyl)-5,6,7,8-tetrahydroacridin-9-amine (4)**. Commercial 1, 4-diaminobutane (264.5 mg, 3.0 mmol, 2.0 equiv.), phenol (0.65 g), NaI (30 mg) and 9-chloro-1,2,3,4-tetrahydroacridine[1] (325.6 mg, 1.5 mmol, 1.0 equiv) were carefully heated at 180 ^oC for 2 h and then allowed to cool down to room temperature. Then the mixture was diluted with EtOAc and alkalinized with 10% KOH solution. The organic layer was washed with brine and dried over $MgSO_4$. Further purification was achieved by column chromatography with an eluent of EtOAc/MeOH=20/1 to give the product *N*-(4-aminobutyl)-5,6,7,8-tetrahydroacridin-9-amine (**4**)[2] 111.4 mg as a light yellow oil. Yield: 28%. ^1H NMR (600 MHz, $CDCl_3$): δ ppm 1.40–1.50 (m, 2 H), 1.57–1.66 (m, 2 H), 1.77–1.87 (m, 4 H), 2.56–2.68 (m, 4 H), 2.98 (t, J = 6.16 Hz, 2 H), 3.40 (t, J = 7.19 Hz, 2 H), 7.25 (ddd, J = 9.10, 6.16, 1.17 Hz, 2 H), 7.46 (ddd, J = 8.44, 6.82, 1.47 Hz, 2 H), 7.83 (dd, J = 8.51, 0.88 Hz, 2 H), 7.88 (dd, J = 8.51, 0.88 Hz, 2 H); ^{13}C NMR (150 MHz, $CDCl_3$): δ ppm 22.6, 22.8, 24.6, 28.9, 30.8, 33.9, 41.6, 49.1, 115.7, 120.0, 122.6, 123.3, 128.0, 128.5, 147.3, 150.4, 158.2.

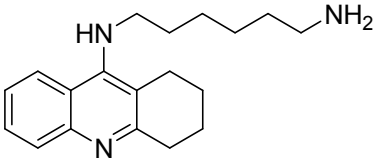

***N*-(6-Aminohexyl)-5,6,7,8-tetrahydroacridin-9-amine (5)**. Following the same procedure as shown above for compound **4**, starting from commercial 1,6-diaminohexane and 9-chloro-1,2,3,4-tetrahydroacridine,[1] compound **5**[1] was isolated (59%) as a light yellow oil: ^{1}H NMR (600 MHz, $CDCl_3$): δ ppm 1.28–1.46 (m, 6 H), 1.60–1.69 (m, 2 H), 1.83–1.94 (m, 4 H), 2.60–2.73 (m, 4 H), 2.99–3.08 (m, 2 H), 3.40–3.52 (m, 2 H), 7.28–7.34 (m, 1 H), 7.48–7.55 (m, 1 H), 7.88 (d, *J* = 8.51 Hz, 1 H), 7.93 (d, *J* = 8.51 Hz, 1 H); ^{13}C NMR (150 MHz, $CDCl_3$): δ ppm 22.7, 23.0, 24.7, 26.6, 26.7, 31.7, 33.4, 33.9, 41.9, 49.4, 115.7, 120.1, 122.8, 123.5, 128.2, 128.5, 147.3, 150.7, 158.3.

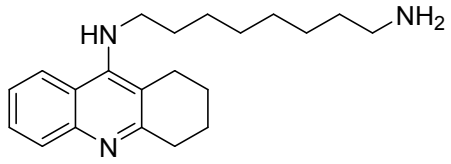

***N*-(8-Aminooctyl)-5,6,7,8-tetrahydroacridin-9-amine (6)**. Following the same procedure as shown above for compound **4**, starting from commercial 1,8-diaminooctane and 9-chloro-1,2,3,4-tetrahydroacridine,[1] compound **6**[1] was isolated (61%) as a light yellow oil: ^{1}H NMR (400 MHz, $CDCl_3$): δ ppm 1.23–1.44 (m, 10 H), 1.54–1.67 (m, 2 H), 1.83–1.92 (m, 4 H), 2.57–2.74 (m, 4 H), 2.97–3.07 (m, 2 H), 3.38–3.50 (m, 2 H), 3.94 (brs., 1 H), 7.31 (ddd, *J* = 8.41, 6.94, 1.27 Hz, 1 H), 7.52 (ddd, *J* = 8.41, 6.85, 1.37 Hz, 1 H), 7.85–7.95 (m, 2 H); ^{13}C NMR (100 MHz, $CDCl_3$): δ ppm 22.7, 23.0, 24.7, 26.7, 26.8, 29.2, 29.3, 31.7, 33.6, 34.0, 42.1, 49.4, 115.7, 120.1, 122.8, 123.4, 128.2, 128.6, 147.4, 150.7, 158.3.

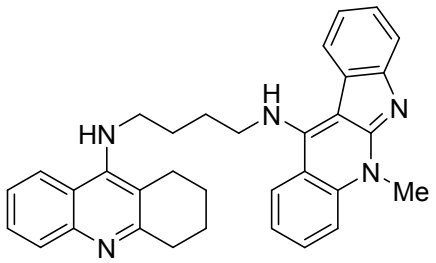

5-Methyl-*N*-(4-(5,6,7,8-tetrahydroacridin-9-ylamino)butyl)-5*H*-indolo[2,3-*b*]quinolin-11-amine (1). The mixture of *N*-(4-aminobutyl)-5,6,7,8-tetrahydroacridin-9-amine (**4**) (111.4 mg, 0.4 mmol, 1.0 equiv) and 11-chloro-5-methyl-5*H*-indolo[2,3-

b]quinolone (**7**)[3] (132.4 mg, 0.5 mmol, 1.2 equiv) was heated at reflux in THF (5 mL) for 12 h and then cooled down to room temperature. The mixture was concentrated under reduced pressure and then purified by column chromatography on silica gel with a eluent from EtOAc to EtOAc/MeOH = 20/1 to give the final product **1** (153.9 mg, 75%) as yellow solid: ^{1}H NMR (600 MHz, $CDCl_3$): δ ppm 1.57–1.65 (m, 2 H), 1.72 (quin, *J* = 7.34 Hz, 2 H), 1.75–1.81 (m, 2 H), 1.81–1.88 (m, 2 H), 2.51 (t, *J* = 6.31 Hz, 2 H), 3.01 (t, *J* = 6.31 Hz, 2 H), 3.34 (q, *J* = 6.75 Hz, 2 H), 3.73 (q, *J* = 6.75 Hz, 2 H), 3.77 (t, *J* = 6.31 Hz, 1 H), 4.18 (s, 3 H), 5.04 (t, *J* = 5.87 Hz, 1 H), 7.16 (t, *J* = 7.80 Hz, 1 H), 7.23–7.29 (m, 2 H), 7.42–7.46 (m, 1 H), 7.50 (ddd, *J* = 8.36, 6.90, 1.17 Hz, 1 H), 7.56 (d, *J* = 8.51 Hz, 1 H), 7.62–7.66 (m, 1 H), 7.76–7.82 (m, 3 H), 7.88 (d, *J* = 8.51 Hz, 1 H), 7.98–8.02 (d, *J* = 8.51 Hz, 1 H); ^{13}C NMR (150 MHz, $CDCl_3$): δ ppm 22.6, 22.8, 24.7, 28.7, 29.3, 32.6, 33.9, 48.7, 48.7, 108.5, 114.6, 115.6, 116.4, 117.4, 118.8, 120.2, 120.4, 120.6, 122.4, 123.7, 123.8, 124.0, 126.0 128.2, 128.7, 130.3, 137.9, 147.3, 148.2, 150.1, 152.8, 156.4, 158.4. HRMS (ESI) Calcd for $C_{33}H_{34}N_5$ $[M+H]^+$ 500.2809. Found 500.2810. Anal. Calcd for $C_{33}H_{33}N_5$: C, 79.33; H, 6.66; N, 14.02. Found: C, 79.54; H, 6.54; N, 14.31.

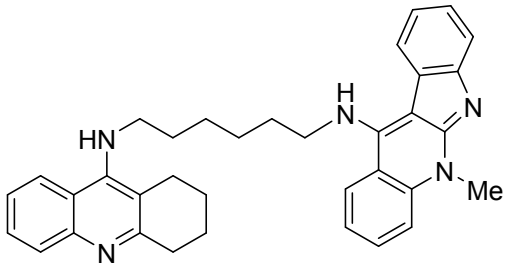

5-Methyl-*N*-(6-(5,6,7,8-tetrahydroacridin-9-ylamino)hexyl)-5*H*-indolo[2,3-*b*]quinolin-11-amine (2). Following the same procedure as shown above for compound **1**, *N*-(6-aminohexyl)-5,6,7,8-tetrahydroacridin-9-amine (**5**) and 11-chloro-5-methyl-5*H*-indolo[2,3-*b*]quinolone (**7**) gave compound **2** (34%) isolated as a yellow solid: ^{1}H NMR (600 MHz, $CDCl_3$): δ ppm 1.27–1.41 (m, 4 H), 1.53 (dt, *J* = 14.45, 7.30 Hz, 2 H), 1.66 (quin, *J* = 7.19 Hz, 2 H), 1.81–1.92 (m, 4 H), 2.61 (t, *J* = 6.02 Hz, 2 H), 3.03 (t, *J* = 6.16 Hz, 2 H), 3.29–3.38 (m, 2 H), 3.68–3.77 (m, 2 H), 3.84 (t, *J* = 5.87 Hz, 1 H), 4.18 (s, 3 H), 5.07 (t, *J* = 5.72 Hz, 1 H), 7.16–7.19 (m, 1 H), 7.29 (t, *J* = 7.63 Hz, 2 H), 7.41–7.45 (m, 1 H), 7.51 (ddd, *J* = 8.36, 6.90, 1.17 Hz, 1 H), 7.57 (d, *J* = 8.51 Hz, 1 H), 7.62–7.67 (m, 1 H), 7.77 (d, *J* = 7.92 Hz, 1 H), 7.82 (d, *J* = 7.63 Hz, 1 H), 7.86 (d, *J* = 8.22 Hz, 1 H), 7.87–7.91 (m, 1 H), 8.05 (dd, *J* = 8.22, 1.17 Hz, 1 H);

^{13}C NMR (150 MHz, $CDCl_3$): δ ppm 22.7, 22.9, 24.6, 26.3, 26.4, 31.4, 31.7, 32.6, 33.9, 49.0, 49.1, 108.0, 114.6, 115.6, 115.9, 117.3, 118.7, 120.1, 120.4, 120.6, 122.6, 123.5, 123.9, 124.2, 125.8, 128.1, 128.6, 130.2, 138.0, 147.3, 148.4, 150.4, 152.7, 156.4, 158.3. HRMS (ESI) Calcd for $C_{35}H_{38}N_5$ $[M+H]^+$ 528.3122. Found 528.3128. Anal. Calcd for $C_{35}H_{37}N_5$: C, 79.66; H, 7.07; N, 13.27. Found: C, 79.57; H, 7.28; N, 13.09.

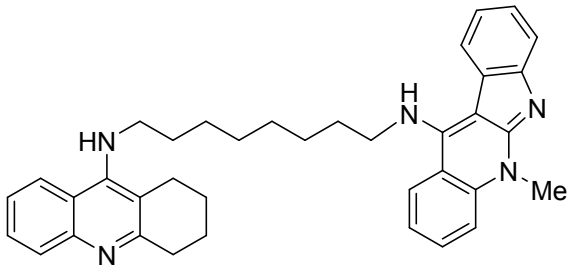

5-Methyl-*N*-(8-(5,6,7,8-tetrahydroacridin-9-ylamino)octyl)-5*H*-indolo[2,3-*b*]quinolin-11-amine (3). Following the same procedure as shown above for compound **1**, *N*-(8-aminooctyl)-5,6,7,8-tetrahydroacridin-9-amine (**6**) and 11-chloro-5-methyl-5*H*-indolo[2,3-*b*]quinolone (**7**) gave compound **3** (65%) isolated as a yellow solid: ^{1}H NMR (600 MHz, $CDCl_3$): δ ppm 1.18–1.32 (m, 6 H), 1.32–1.41 (m, 2 H), 1.53–1.61 (m, 2 H), 1.71 (quin, *J* = 7.34 Hz, 2 H), 1.84–1.93 (m, 4 H), 2.67 (t, *J* = 5.14 Hz, 2 H), 3.05 (t, *J* = 5.58 Hz, 2 H), 3.39–3.46 (m, 2 H), 3.75–3.84 (m, 2 H), 3.93 (brs., 1 H), 4.21–4.28 (s, 3 H), 5.13 (t, *J* = 5.28 Hz, 1 H), 7.19 (t, *J* = 7.34 Hz, 1 H), 7.29–7.36 (m, 2 H), 7.44 (t, *J* = 7.63 Hz, 1 H), 7.53 (dd, *J* = 8.22, 7.04 Hz, 1 H), 7.63–7.67 (m, 1 H), 7.67–7.72 (m, 1 H), 7.78 (d, *J* = 7.92 Hz, 1 H), 7.86 (d, *J* = 7.92 Hz, 1 H), 7.91 (t, *J* = 9.54 Hz, 2 H), 8.11–8.15 (m, 1 H); ^{13}C NMR (150 MHz, $CDCl_3$): δ ppm 22.7, 23.0, 24.7, 26.5, 26.6, 29.0, 29.0, 31.6, 31.9, 32.7, 33.9, 49.2, 49.3, 108.1, 114.7, 115.7, 117.4, 118.8, 120.1, 120.4, 120.6, 122.8, 123.5, 123.9, 124.4, 125.9, 128.2, 128.6, 130.3, 138.1, 147.3, 148.6, 150.7, 152.7, 156.4, 158.3. HRMS (ESI) Calcd for $C_{37}H_{42}N_5$ $[M+H]^+$ 556.3435. Found 556.3436. Anal. Calcd for $C_{37}H_{41}N_5$: C, 79.96; H, 7.44; N, 12.60. Found: C, 79.77; H, 7.28; N, 12.87.

2. Biological evaluation

2.1. Inhibition of human AChE and BuChE. The capacity of **1-3** to inhibit human ChE activity was assessed using the Ellman's assay.[4] A Jasco V-530 double beam spectrophotometer connected to a HAAKE DC30 thermostating system (Thermo Haake, Germany) was used. Stock solutions of the tested compound (1-2 mM) were prepared in methanol and diluted in methanol. The assay solution consisted of a 0.1 M phosphate buffer, pH 8.0, with the addition of 340 μM 5,5'-dithiobis(2-nitrobenzoic acid), 0.02 unit/mL human recombinant AChE or BuChE from human serum (Sigma-Aldrich, Italy), and 550 μM substrate, i.e., acetylthiocholine iodide or butyrylthiocholine iodide, respectively (Sigma-Aldrich, Italy). Tested compounds were added to the assay solution at increasing concentrations and preincubated at 37°C with the enzyme for 20 min before the addition of substrate. The rate of absorbance increase at 412 nm was followed for 5 min. In parallel, blanks containing all components except the enzyme were prepared to account for the non enzymatic hydrolysis of the substrate. The reaction rates were compared and the percent inhibition due to the presence of test compounds was calculated. Each concentration was analyzed in duplicate/triplicate. The percent inhibition of the enzyme activity due to the presence of inhibitor was calculated. Inhibition plots were obtained for each compound by plotting the percent inhibition versus the logarithm of inhibitor concentration in the assay solution. The linear regression parameters were determined for each curve and the IC_{50} extrapolated.

2.2. Determination of the inhibitory effect on the $A\beta_{42}$ self-aggregation by thioflavin T fluorometric assay. 1,1,1,3,3,3-Hexafluoro 2-propanol pretreated $A\beta_{42}$ samples (Bachem AG, Switzerland) were resolubilized with a CH_3CN/0.3 mM Na_2CO_3/250 mM NaOH (48.4/48.4/3.2) mixture to have a stable stock solution ([Aβ] = 500 μM).[5] Experiments were performed by incubating the peptide in 10 mM phosphate buffer (pH = 8.0) containing 10 mM NaCl, at 30 °C for 24 h ([$A\beta_{42}$]= 50 μM) with and without the tested compound at 10 μM ($A\beta_{42}$/inhibitor = 5/1). To quantify amyloid fibril formation, the thioflavin T method was used.[6,7] After incubation, samples were diluted to a final volume of 2.0 mL with 50 mM glycine-NaOH buffer (pH 8.5) containing 1.5 μM thioflavin T. A 300-seconds-time scan of fluorescence intensity was carried out (λ_{exc} = 446 nm; λ_{em} = 490 nm) using a Jasco FP-6200 spectrofluorometer (Jasco

Europe) and values at plateau were averaged after subtracting the background fluorescence of the 1.5 μM thioflavin T solution. Percent inhibition was calculated by comparing corrected signal obtained in the absence and in the presence of inhibitor.
All tested compounds showed a significant quenching of the thiofalvin T signal generated in the presence of preformed amyloid fibrils. The % quenching was determined and subtracted while calculating the inhibitory activity.

2.3. The hepatotoxicity of tacrine-neocryptolepines 1-3

2.3.1. *In vitro* model and cell culture conditions

The human hepatoma cell line HepG2 was kindly provided by IdiPAZ Institute for Health Research (Madrid, Spain). These cells were cultured in Eagle´s minimum essential medium (EMEM) supplemented with 15 nonessential amino acids, 1 mM sodium pyruvate, 10% heat-inactivated fetal bovine serum (FBS) and 100 units/mL penicillin, and 100 μg/mL streptomycin (reagents from Invitrogen, Madrid, Spain). Cultures were seeded into flasks containing supplemented medium and maintained at 37 ºC in a humidified atmosphere of 5% CO_2 and 95% air. Culture media were changed every 2 days. Cells were sub-cultured after partial digestion with 0.25% trypsin-EDTA. For test, HepG2 cells were sub-cultured in 96-well plates at a seeding density of $1x10^5$ cells per well. When the HepG2 cells reached 80% confluence, the medium was replaced with fresh medium containing 1-300 μM compounds (1-3 and tacrine used as reference) or 0.1% DMSO used as a vehicle control.

2.3.2. Measurement of cell viability

Cell viability was determined by quantitative colorimetric assay with 3-[4,5 dimethylthiazol-2-yl]-2,5-diphenyl-tetrazolium bromide (MTT). Briefly, 50 μL of the MTT labeling reagent, at a final concentration of 0.5 mg/mL, was added to each well at the end of the incubation period and the plate was placed in a humidified incubator at 37 ºC with 5% CO_2 and 95% air (v/v) for an additional 2 h period. Metabolically active cells convert the yellow MTT tetrazolium compound to a purple formazan product. Then, the insoluble formazan was dissolved with DMSO; colorimetric determination of MTT reduction was measured in an ELISA microplate reader at 540 nm. Control cells treated with EMEM were taken as 100 % viability.

3. Docking analysis

3.1. Experimental methods

Molecular docking into AChE and and BuChE. Compounds **1-3** were assembled within Discovery Studio, version 2.1, software package, using standard bond lengths and bond angles. With the CHARMm force field[8] and partial atomic charges, the molecular geometries of **1, 2** and **3** were energy-minimized using the adopted-based Newton-Raphson algorithm. Structures were considered fully optimized when the energy changes between iterations were less than 0.01 kcal/mol mol.[9]

3.2. Docking of compounds 1-3 into hAChE and hBuChE

The coordinates of hAChE (PDB ID: 1B41), were obtained from the Protein Data Bank (PDB). For docking studies, initial protein was prepared by removing all water molecules, heteroatoms, any co-crystallized solvent and the ligand. Proper bonds, bond orders, hybridization and charges were assigned using protein model tool in Discovery Studio, version 2.1, software package. CHARMm force field was applied using the receptor-ligand interactions tool in Discovery Studio, version 2.1, software package. Docking calculations were performed with the program Autodock Vina.[10] AutoDockTools (ADT; version 1.5.4) was used to add hydrogens and partial charges for proteins and ligands using Gasteiger charges. Flexible torsions in the ligands were assigned with the AutoTors module, and the acyclic dihedral angles were allowed to rotate freely. Trp286, Tyr124, Tyr337, Tyr72, Asp74, Thr75, Trp86, and Tyr341 receptor residues were selected to be flexible during docking simulation using the AutoTors module. The box center was defined and the docking box was displayed using ADT. The docking procedure was applied to the whole protein target, without imposing the binding site ("blind docking"). A grid box of 60 x 60 x 72 with grid points separated 1 Å, was positioned at the middle of the protein (x = 116.546; y = 110.33; z = -134.181). Default parameters were used except num_modes, which was set to 40. The AutoDock Vina docking procedure used was previously validated.[11]

The three-dimensional structure of hBuChE has been used (PDB ID: 4BDS). Proper bonds, bond orders, hybridization and charges were assigned using protein model tool in Discovery Studio, version 2.1, software package. CHARMm force field was applied using the receptor-ligand interactions tool in Discovery Studio. Docking calculations

were performed following the same protocol described before for hAChE. All dockings were performed as blind dockings where a box of 66 x 66 x 70 Å with grid points separated 1 Å, was positioned at the middle of the protein (x=136.0; y=123.59; z=38.56). Default parameters were used except num_modes, which was set to 40. The lowest docking-energy conformation was considered as the most stable orientation. Finally, the docking results generated were directly loaded into Discovery Studio, version 2.1. Two dimensional figures of the **1-3**-enzymes interactions were groodmed using DS 2.1.

3.3. Docking analysis on hBuChE

Compounds **1-3** were modeled into the structure of hBuChE (PDB: 4BDS) and all the experiments were performed as blind dockings following the same computational protocol used for hAChE.

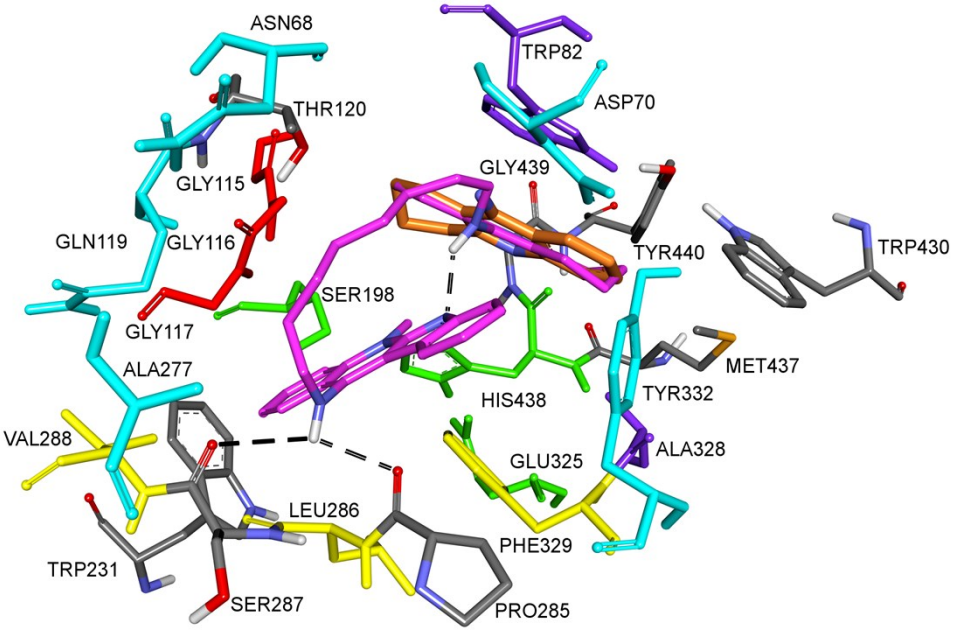

Figure 1S. Proposed binding mode for compound 3 inside gorge cavity of hBuChE superimposed with the binding mode showed by tacrine. Compound **3** is colored pink. Tacrine is shown as orange sticks instead of lime green sticks. Different subsites of the active site were colored: catalytically anionic site (CAS) in green, oxyanion hole (OH) in red, choline binding site in violet (CBS), acyl binding pocket (ABP) in yellow, and peripheral site (PAS) in blue. Hydrogen bonds are indicated with black dashed lines.

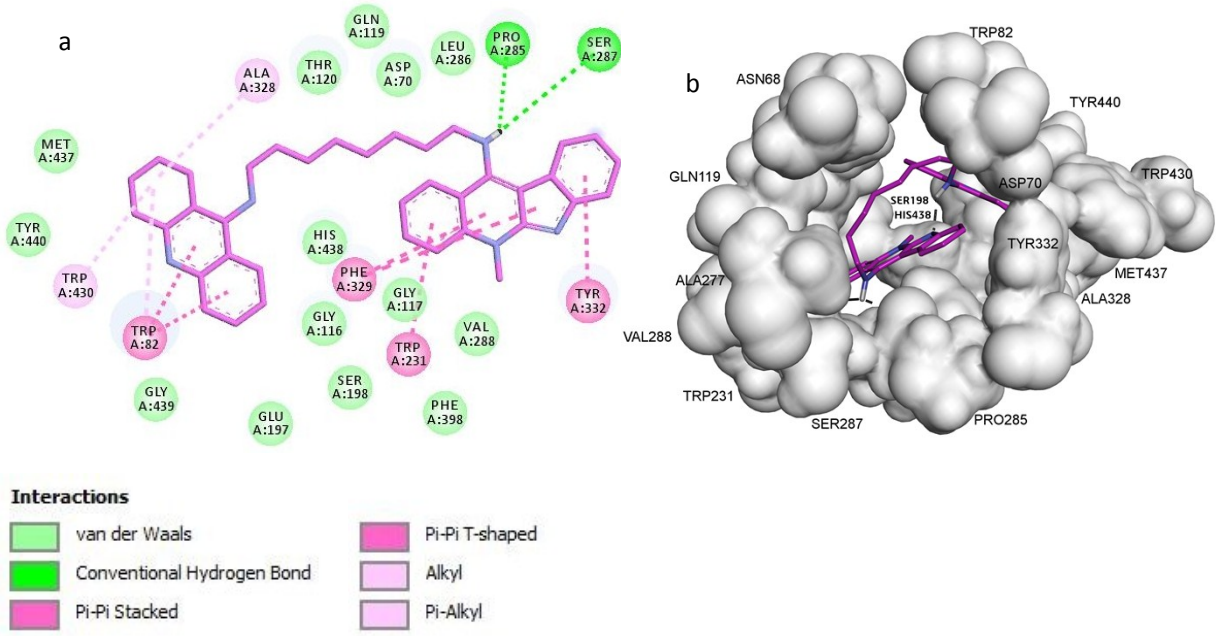

Figure 2S. a) Schematic representation of different interactions of compound **3** with hBuChE. b) External surface with the gorge cavity of hBuChE showing the proposed binding mode for compound **3**.

The best-ranked docking solutions revealed that hBuChE could effectively accommodate compound **3** inside the active site gorge. Thus, compound **3** interacts inside hBuChE binding cavity in the same region occupied by tacrine co-crystalized with hBuChE (PDB: 4BDS) (Figure 1S). This compound finds interactions in the middle of the active-site gorge and tacrine moiety is pointed toward the catalytic triad residues, His438, Ser198 and Glu325.

The **3**-BuChE complex was stabilized mainly by hydrophobic interactions. Other interactions to consider would be the hydrogen bonds established between Pro285 and Ser287 and the NH group of the ligand. Docking simulations also suggest a face-to-face interaction between the tacrine moiety of the ligand and the side chain of Trp82 (Figures 2Sa and 2Sb). Moreover, compound **3** is showing a NH group that can establish an intramolecular interaction with the nitrogen atom of the benzimidazole moiety of the ligand (Figure 1S).

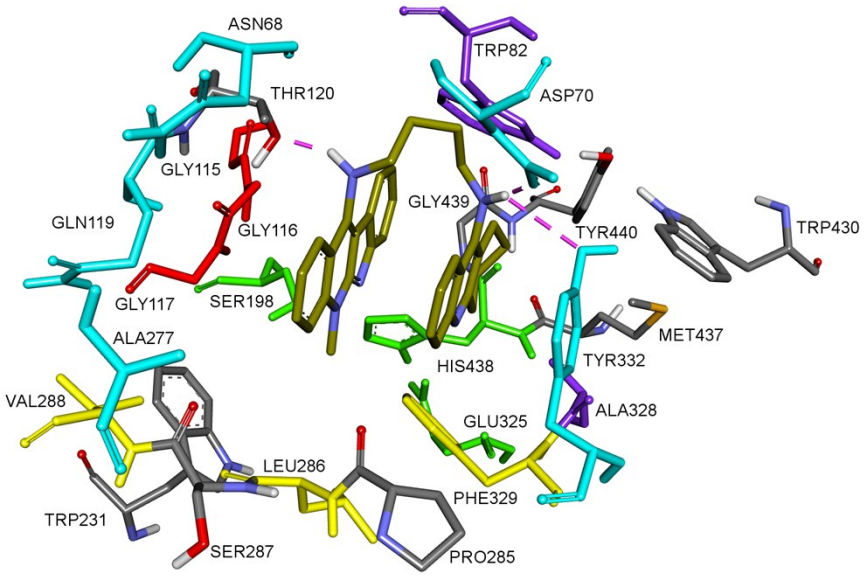

Figure 3S. Proposed binding mode for compound 1 inside gorge cavity of hBuChE. Compound **1** is colored olive green. Different subsites of the active site were colored: catalytically anionic site (CAS) in green, oxyanion hole (OH) in red, choline binding site in violet (CBS), acyl binding pocket (ABP) in yellow, and peripheral site (PAS) in blue. Hydrogen bonds are indicated with pink dashed lines.

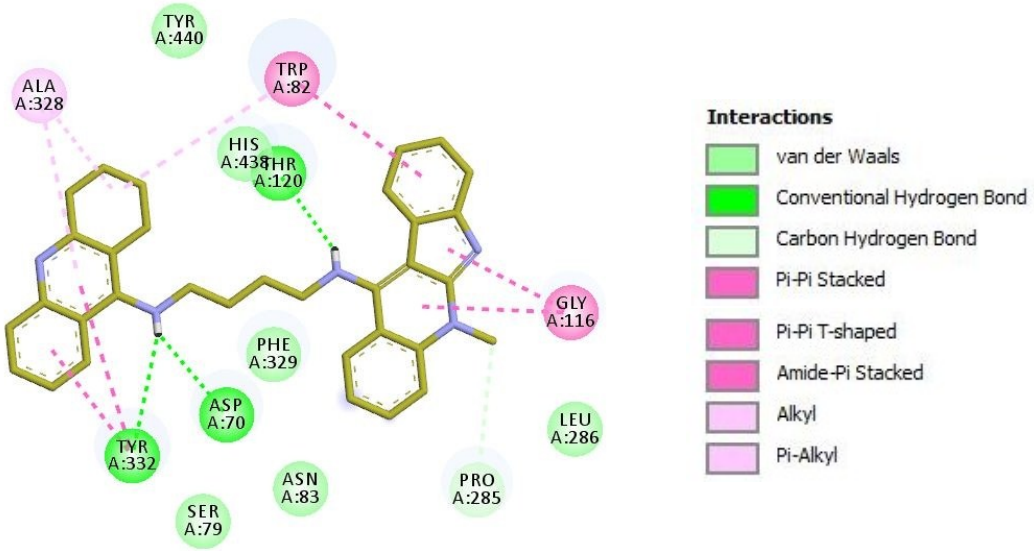

Figure 4S. Schematic representation of different interactions of compound 1 with hBuChE

Compound **1** fits into the active site of hBuChE through π–π and hydrogen bonds interactions, which are found to be essential for binding. As shown in figure 3S it was found that the tacrine moiety occupied the catalytic site of hBuChE through π–π stacking interactions with Tyr332. Furthermore, the binding is also supported by the formation of hydrogen bond between a NH group of the ligand and Thr120. In addition

at the beginning of the gorge the NH group of substituted tacrine established hydrogen bond interactions with Asp70 and Tyr332 (key residues of PAS). Neocryptolepine motif makes π–π T-shaped interaction with Trp82 of choline binding site and it also makes amide-π stacked interaction with Gly116 of oxyanion hole of CS (Figure 4S).

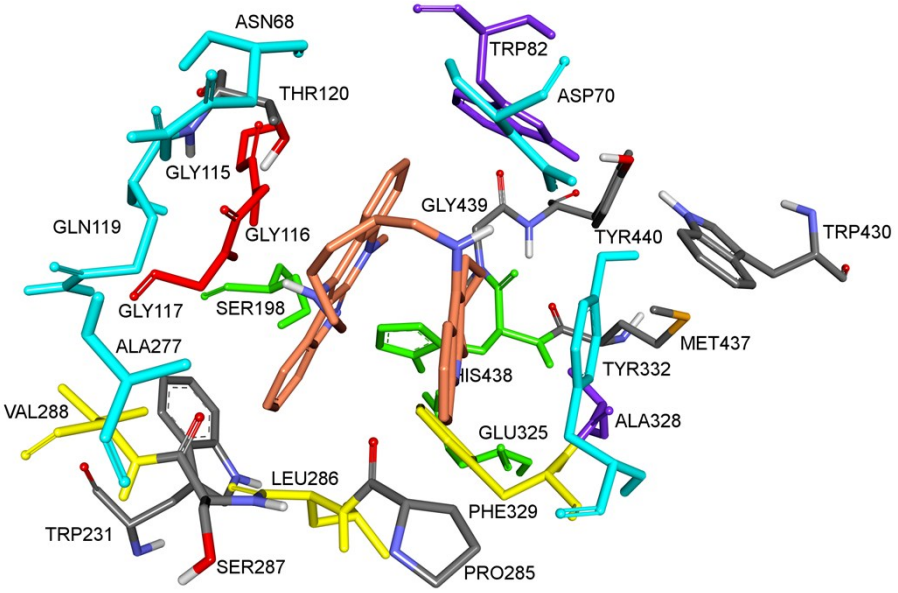

Figure 5S. Proposed binding mode for compound 2 inside gorge cavity of hBuChE. Compound **2** is colored orange. Different subsites of the active site were colored: catalytically anionic site (CAS) in green, oxyanion hole (OH) in red, choline binding site in violet (CBS), acyl binding pocket (ABP) in yellow, and peripheral site (PAS) in blue.

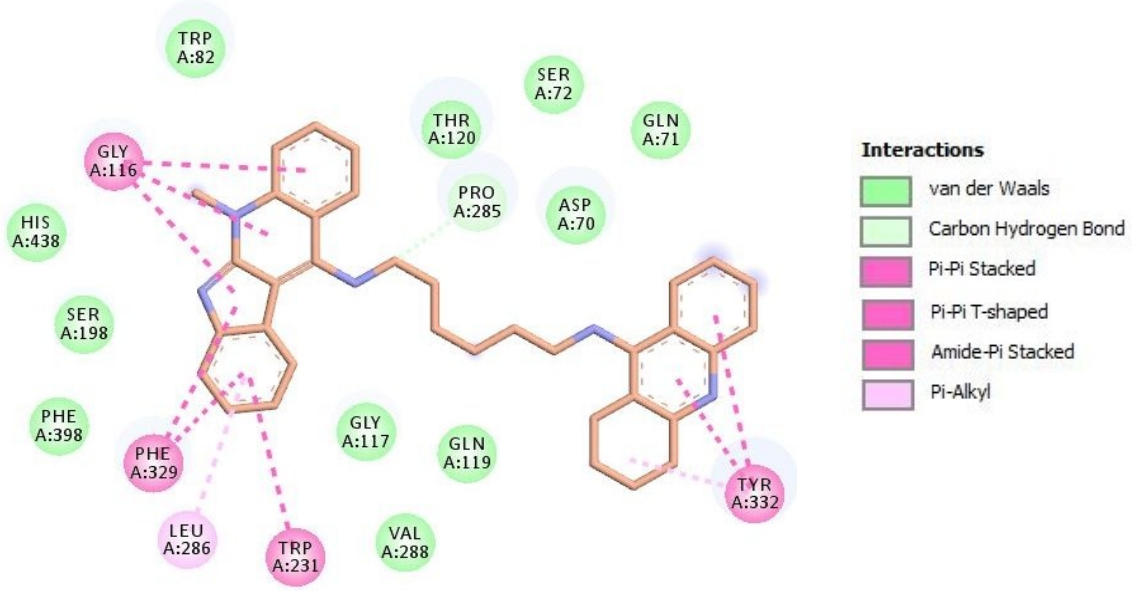

Figure 6S. Schematic representation of different interactions of compound 2 with hBuChE.

On the other hand, molecular docking of compound **2** in the active site of hBuChE has been shown in figure 5S. Tacrine moiety of compound **2** makes π–π stacking interaction with Tyr332 of PAS. Also, polymethylene linker placed in the vicinity of Asp70 and Gln119 (key residues of PAS) and van der Waals interactions were established (Figure 6S)

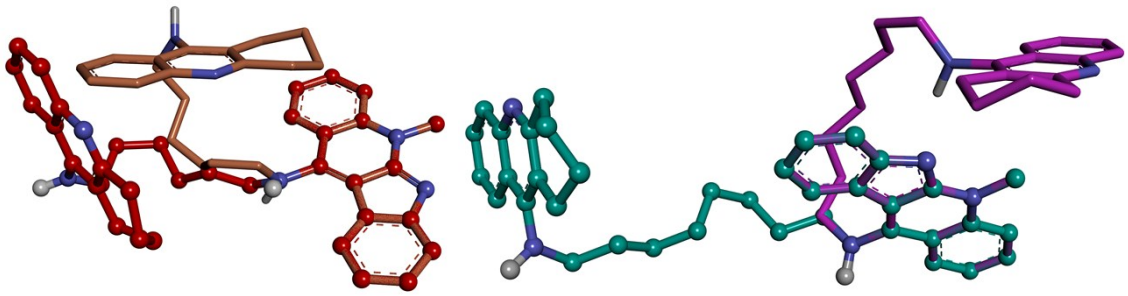

Fig 7S. a) Superposition of the bioactive conformations for compound **2** in hAChE (red balls and sticks) and in hBuChE (orange sticks). b) Superposition of the bioactive conformations for compound **3** in hAChE (green balls and sticks) and in hBuChE (pink sticks)

The binding mode of compound **1** in the hAChE active site is not very different from the binding mode in the hBuChE active site. However, the orientations and conformations of compounds **2** and **3** in AChE were completely different from those in hBuChE. These ligands bind to hAChE with extended conformations whereas they bind to hBuChE with folded conformations (Figure 7S). The docking calculations of compounds **1**, **2** and **3** at the active sites of hAChE and hBuChE revealed that the compounds bound to the hAChE enzyme with lower binding energy when compared with hBuChE enzyme. The energy gaps in hBuChE are approximately 0.3, 2.9 and 2.1 kcal/mol (for compounds **1**, **2** and **3**, respectively) higher than the calculated for the hAChE. The values of 2.9 and 2.1 Kcal/mol for the energetic penalties in compounds **2** and **3** can be, at least in part, the reason for why compound **2** is quite more selective than **3** for the inhibition of hAChE.

4. ADME of tacrine-neocryptolepine derivatives 1-3

Table 1S. Physicochemical properties for compounds **1-3** calculated using Qikprop

Molecule	MW	SASA	volume	donorHB	accptHB	QPlogPo/w	QPlogS
1	525.863	770.792	1.565.973	4.000	8.000	2.415	0.134
2	553.916	818.114	1.679.559	4.000	8.000	3.081	-0.317
3	581.970	923.011	1.826.261	4.000	8.000	3.973	-1.758

Molecule	QPPCaco	PSA	QPlogBB	metab	QPlogKhsa	% HOA	ROF	ROT
1	62.274	44.966	0.553	4	0.888	60.244	1	0
2	58.055	44.589	0.392	4	1.081	63.596	1	0
3	64.499	45.586	0.265	4	1.325	69.636	1	0

MW: Molecular weight of the molecule (130.0-725.0). SASA: Total Solvent Accessible Surface Area, in square angstroms, using a probe with a 1.4Å radius (limits 300.0-1000.0). volume: Total solvent-accessible volume, in cubic angstroms, using a probe with a 1.4 Å radius (limits 500.0-2000.0). donorHB: Estimated number of hydrogen bonds that would be accepted by the solute (limits: 2.0-20.0). accptHB: Estimated number of hydrogen bonds that would be donated by the solute (limits: 0.0-6.0). QPlogPo/w: Predicted octanol/water partition coefficient (limits -2.0-6.5). QPlogS: Predicted aqueous solubility. S, in mol/dm^3, is the concentration of the solute's saturated solution that is in equilibrium with crystalline solid (limits -6.5-0.5). QPPCaco: Predicted apparent Caco-2 cell permeability in nm/sec. Caco-2 cells are a model for the gut-blood barrier. QikProp predictions are for non-active transport. (< 25 poor, > 500 great). PSA: Van der Waals surface area of polar nitrogen and oxygen atoms (limits 7.0-200.0). QPlog BB- Predicted brain/blood partition coefficient (limits -3.0–1.2). metab: Number of likely metabolic reactions (limits 1-8). QPlogKhsa: Prediction of binding to human serum albumin (limits -1.5-1.5). HOA: Predicted qualitative Human Oral Absorption on 0 to 100% scale. ROF: Number of violations of Lipinski's Rule Of Five (Lipinski, C. A., Lombardo, F., Dominy, B. W., Feeney, P. J., "Experimental and computational approaches to estimate solubility and permeability in drug discovery and development settings", *Adv. Drug Delivery rev*. **2001**, 46, 3-26). (molecular weight < 500, QPlogPo/w < 5,number of hydrogen bond donor ≤ 5, number of hydrogen bond acceptors HB ≤ 10). ROT: Number of violations of Jorgensen's rule of three [(a) Duffy, E. M., Jorgensen,W. L., "Prediction of Properties from Simulations: Free Energies of Solvation in Hexadecane, Octanol, and Water", *J. Am. Chem. Soc.* 2000, 122, 2878-2888; (b) Jorgensen, W. L., Duffy, E. M., "Prediction of Drug Solubility from Monte Carlo Simulations", *Bioorg. Med. Chem. Lett*. **2000**, 10, 1155-1158](QPlogS> -5.7, QPCaco> 22 nm/s, number of primary metabolites < 7).

5. Inhibition of amyloid self-aggregation

Table 2S. Experimental values for the $A\beta_{1-42}$ self-aggregation as determined by the ThT-based fluorescence assay.

	IF exp1	IF exp2	% exp1	% exp2	% inhib average	% quenching	% inhib corr
$A\beta_{1-42}$ 50 µM	5,042	5,3035					
bis(7)tacrine 10 µM	2,4812	2,3298	50,8	56,1	53,4	0,0	**53,4**
Cmpd 1, 10 µM	2,6494	2,4989	47,5	52,9	50,2	30,5	**19,7**
Cmpd 2, 10 µM	2,1301	2,3828	57,8	55,1	56,4	30,5	**25,9**
Cmpd 3, 10 µM	2,4464	2,008	51,5	62,1	56,8	30,3	**26,5**
Tacrine, 10 µM	4,9228	4,9976	2,2	5,8	4,0	0,0	**4,0**

IF = intensity of fluorescence (arbitrary units) after a 300s scan.

6. References

1 P. R. Carlier, D.-M. Du, Y. Han, J. Liu and Y.-P. Pang, *Bioorg. Med. Chem. Lett.,* 1999, **9**, 2335-2338.

2 J.-S. Lan, S.-S. Xie, L., S.-Y. Li, L.-F. Pan, X.-B. Wang and L.-Y. Kong, *Bioorg. Med. Chem.,* 2014, **22**, 6089-6104.

3 L. Wang, M. Switalska, Z.-W. Mei, W.-J. Lu, Y. Takahara, X.-W. Feng, I. E-T. El-Sayed, J. Wietrzyk and T. Inokuchi, *Bioorg. Med. Chem.,* 2012, **20**, 4820-4829.

4 G. L. Ellman, K. D. Courtney, V. Andres Jr. and R. M. Feather-Stone, *Biochem. Pharmacol.,* 1961, **7**, 88-95.

5 M. Bartolini, C. Bertucci, M. L. Bolognesi, A. Cavalli, C. Melchiorre and V. Andrisano, *ChemBioChem,* 2007, **8**, 2152-2161.

6 H. Naiki, K. Higuchi, K. Nakakuki and T. Takeda, *Lab. Invest.,* 1991*,* **65**, 104-110.

7 H. LeVine, *Protein Sci.,* 1993*,* **2**, 404-410.

8 B. R. Brooks, R. E. Bruccoleri, B. D. Olafson, D. J. States, S. Swaminathan and M. Karplus, *J. Comput. Chem.,* 1983, **4**, 187–217.

9 A. Morreale, F. Maseras, I. Iriepa and E. Gálvez, *J. Mol. Graphics Model.,* 2002, **21**, 111-118.

10 O. Trott and A. J. Olson, *J. Comput. Chem.*2010, **31**,455–46.

11 M. Bartolini, M. Pistolozzi, V. Andrisano, J. Egea, M. G. López, I. Iriepa, I. Moraleda, E. Gálvez, J. Marco-Contelles and A.Samadi, *ChemMedChem*, 2011, **6**, 1990-1997.